Dalton
Transactions

Cite this: *Dalton Trans.*, 2012, **41**, 4789

www.rsc.org/dalton

PAPER

Synthesis and structures of cyclic gold complexes containing diphosphine ligands and luminescent properties of the high nuclearity species†

Suresh Bhargava,*[a] Kunihiko Kitadai,[b] Takahashi Masashi,[b] Daniel W. Drumm,[a,c] Salvy P. Russo,[a,c] Vivian Wing-Wah Yam,[d] Terence Kwok-Ming Lee,[d] Jörg Wagler[e] and Nedaossadat Mirzadeh[a]

Received 12th September 2011, Accepted 24th January 2012
DOI: 10.1039/c2dt11722c

A mixture of cyclic gold(I) complexes $[Au_2(\mu\text{-}cis\text{-dppen})_2]X_2$ (X = OTf **1**, PF_6 **3**) and $[Au(cis\text{-dppen})_2]X$ (X = OTf **2**, PF_6 **4**) is obtained from the reaction of $[Au(tht)_2]X$ (tht = tetrahydrothiophene) with one equivalent of *cis*-dppen [dppen = 1,2-bis(diphenylphosphino)ethylene]. The analogous reaction with *trans*-dppen or dppa [dppa = bis(diphenylphosphino)acetylene] affords the cyclic trinuclear $[Au_3(\mu\text{-}trans\text{-dppen})_3]X_3$ (X = OTf **11**, PF_6 **12**) and tetranuclear $[Au_4(\mu\text{-dppa})_4]X_4$ (X = OTf **13**, PF_6 **14**, ClO_4 **15**) gold complexes, respectively. Recrystallization of **15** from CH_2Cl_2/MeOH yielded a crystal of the octanuclear gold cluster $[Au_8Cl_2(\mu\text{-dppa})_4](ClO_4)_2$ **16**. Attempts to prepare dicationic binuclear gold(II) species from the reaction of a mixture of **3** and **4** with halogens gave a mixture of products, the components of which confirmed to be acyclic binuclear gold(I) $[Au_2X_2(cis\text{-dppen})]$ (X = I **5**, Br **7**) and cyclic mononuclear gold (III) $[AuX_2(cis\text{-dppen})]PF_6$ (X = I **6**, Br **8**) complexes. Complexes **11–14** reveal weak emission in butyronitrile glass at 77 K, but they are non-emissive at room temperature. *Ab initio* modelling was performed to determine the charge state of the gold atoms involved. Extensive structural comparisons were made to experimental data to benchmark these calculations and rationalize the conformations.

Introduction

There has been remarkable interest in the synthesis and properties of metallomacrocycles, constructed through coordination-directed self-assembly of metal centers and multidentate ligands, or self-assembly through non-covalent interactions. These synthetic strategies have allowed the design and isolation of catenanes, rotaxanes and knots.[1–3] Gold chemistry has contributed a great deal to the broad field of metallomacrocycles[4–11] exhibiting particular promise as optical materials.[12–14] Linear coordination[11,15–17] and aurophilic interactions between metal centres are two leading factors for the use of gold complexes in the formation of complex molecular structures by self-assembly.[11,15,18–23] The factors that influence the formation of the cyclic gold complexes and catenanes have also been investigated, with one factor being the size of the ring formed. Treating a polymeric gold acetylide complex with $Ph_2P(CH_2)_nPPh_2$ (n = 2) gave a discrete cyclic species, while larger phosphines (n = 4, 5) gave only catenanes; when n = 3, a mixture of both species was obtained.[24]

Ditertiaryphosphine ligands are known to act as chelating or bridging groups to form cyclic gold complexes[11] and a number of binuclear compounds have been prepared.[25–30] The geometry of the diphosphine ligand can also play an important role in the formation of metal complexes. For example, treatment of a solution of sodium tetrachloroaurate with one equivalent of *cis*-dppen gives the binuclear complex $[Au_2Cl_2(cis\text{-dppen})]$ in which the diphosphine ligand bridges two metal centers. In contrast, the analogous reaction using *trans*-dppen gives the mononuclear complex $[AuCl(trans\text{-dppen})]$, in which only one of the phosphine centres is coordinated.[31] Recently, the structure of $[Au_2(cis\text{-dppen})_2](NO_3)_2$ has been reported, the crystals of which contain discrete voids capable of capturing and releasing gas molecules.[32]

Polynuclear gold complexes containing diphosphine ligands have been shown to exhibit interesting photophysical properties. The binuclear gold compound $[Au_2(dppm)_2](ClO_4)_2$ [dppm = bis(diphenylphosphino)methane] shows a long-lived emission at 565 nm in acetonitrile and a number of organic halides have been found to quench its emission in acetonitrile.[33] Reaction of dppm with $[Au(C{\equiv}CPh)]_\infty$ in ethanol affords $[Au_3(\mu_2\text{-dppm})_2(C{\equiv}CPh)_2][Au(C{\equiv}CPh)_2]$ which is photoluminescent in the solid state and in solution.[34] The binuclear and trinuclear gold(I) complexes containing dmpm [dmpm = bis

---

[a] *Advanced Materials & Industrial Chemistry, School of Applied Sciences, RMIT University, GPO Box 2476V, Melbourne, Victoria3001, Australia. E-mail: Suresh.bhargava@rmit.edu.au*
[b] *Department of Chemistry, Toho University, Chiba, Japan*
[c] *Applied Physics, School of Applied Sciences, RMIT University, GPO Box 2476V, Melbourne, Victoria3001, Australia*
[d] *Institute of Molecular Functional Materials (Areas of Excellence Scheme, University Grants Committee (Hong Kong)), and Department of Chemistry, The University of Hong Kong, Pokfulam Road, Hong Kong, PR China*
[e] *Institut für Anorganische Chemie, Technische Universität Bergakademie, Freiberg D-09596, Germany*

† Electronic supplementary information (ESI) available. CCDC numbers 843620–843626. For ESI and crystallographic data in CIF or other electronic format see DOI: 10.1039/c2dt11722c

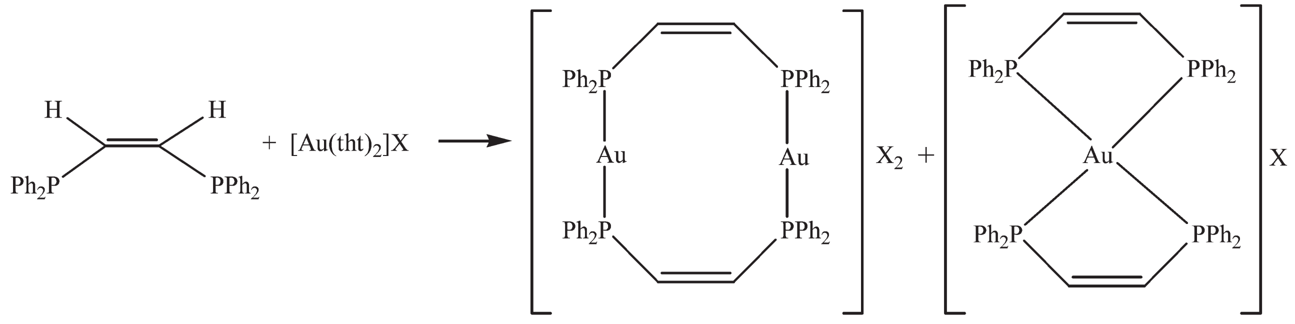

X = OTf **1**, PF$_6$ **3**

X = OTf **2**, PF$_6$ **4**

Scheme 1 Reaction of [Au(tht)$_2$]X (X = OTf, PF$_6$) with one equivalent of *cis*-dppen.

(dimethylphosphino)methane] [Au$_2$(dmpm)$_2$](ClO$_4$)$_2$ and dmmp [dmmp = bis(dimethylphosphinomethyl)methylphosphine] [Au$_3$(dmmp)$_2$](ClO$_4$)$_3$ have been reported to exhibit intriguing emission properties.[35]

In view of this varied behaviour of dppen, we were interested in further exploring its use as a ligand for the formation of gold complexes. The use of the related alkyne analogue of dppen, bis(diphenylphosphino)acetylene, was also investigated and the photoluminescence behaviour of the products was studied.

Results and discussions

Cyclic mono- and binuclear gold complexes

The reaction of [Au(tht)$_2$]OTf with one equivalent of *cis*-dppen (Scheme 1) gave an air- and moisture-stable pale yellow powder, the ^{31}P NMR spectrum of which showed two singlet resonances at δ 23.1 and 25.1, suggesting the presence of two species. Slow recrystallization of this solid gave a mixture of colorless and yellow crystals, identified by X-ray crystallography to be cyclic binuclear gold(I) complex [Au$_2$(μ-*cis*-dppen)$_2$](OTf)$_2$ (**1**) and tetrahedrally coordinated mononuclear gold(I) complex [Au(*cis*-dppen)$_2$]OTf (**2**), respectively. The molecular structure of **1**, which is analogous to [Au$_2$(*cis*-dppen)$_2$](NO$_3$)$_2$,[32] is shown in Fig. 1; selected bond lengths and angles are summarized in the caption to Fig. 1. The ^{31}P NMR spectrum of the isolated solid resulting from the reaction of [Au(tht)$_2$]PF$_6$ with one equivalent of *cis*-dppen showed identical resonances. By analogy to the triflate analogues **1** and **2**, these resonances were assigned to [Au$_2$(μ-*cis*-dppen)$_2$]PF$_6$ (**3**) and [Au(*cis*-dppen)$_2$]PF$_6$ (**4**) (Scheme 1). Complex **4** has been previously reported by Berners-Price *et al.*, and was obtained as a pure compound from the thiodiglycol reduction of Na[AuCl$_4$] in the presence of *cis*-dppen and NH$_4$PF$_6$.[36]

Complex **1** contains two linearly coordinated gold(I) atoms bridged by the dppen ligands, forming a ten-membered ring consisting of two gold, four phosphorus and four ethylenic carbon atoms.

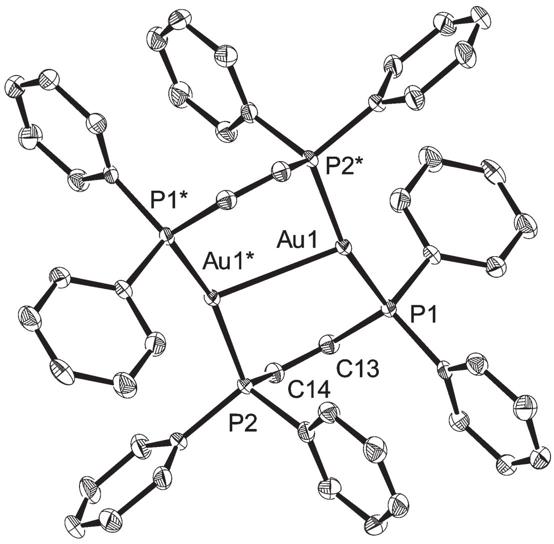

Fig. 1 Molecular structure of **1**. Ellipsoids show 70% probability levels. Hydrogen atoms and OTf counterion have been omitted for clarity. Selected bond distances (Å) and angles (°) in **1**. Au(1)···Au(1*) 2.9802(2), Au(1)–P(1) 2.2937(6), Au(1)–P(2*) 2.3172(6), P(1)–C(13) 1.812(3), P(2)–C(14) 1.810(3), C(13)–C(14) 1.333(4); C(14)–P(2)–Au(1*) 119.17(9), C(14)–C(13)–P(1) 126.5(2), P(1)–Au(1)–Au(1*) 108.115(17), P(1)–Au(1)–P(2*) 161.95(2), P(2*)–Au(1)–Au(1*) 84.561(16). Labels with an asterisk denote atoms at an equivalent position (−*x*, 1 − *y*, 1 − *z*) generated by inversion symmetry.

The Au···Au distance of 2.9802(2) Å in **1** is characteristic of an aurophilic interaction[37] and is slightly longer than the corresponding separation in [Au$_2$(*cis*-dppe)$_2$](NO$_3$)$_2$ [2.904(2) Å],[32] Au$_2$(μ-dppm)$_2$Cl$_2$ [2.962(1) Å],[26] [Au$_2${μ-(2-C$_6$H$_3$-6-Me)PPh$_2$}$_2$] [2.861(2) Å][38] and [Au$_2$(μ-dppe)$_2$](OTf)$_2$ [2.9594(10) Å].[39] The Au–P distances of 2.2937(6) Å and 2.3172(6) Å are almost identical to the bonds in [Au$_2${μ-(2-C$_6$H$_3$-6-Me)PPh$_2$}$_2$] [2.302(2) Å and 2.295(2) Å][38] and [Au$_2$(*cis*-dppe)$_2$](NO$_3$)$_2$ [2.303(2)–2.324(2) Å]. The P–Au–P angle [161.95(2)°] is considerably distorted from linear coordination, most likely as a consequence of aurophilic interaction.

Reactions with halogens

There is an ever growing family of binuclear gold(II) complexes containing metal–metal bonds being reported in literature,[40] however dicationic digold(II) species are extremely rare; the only reported examples being [Au$_2$X$_2$(dppam)$_2$][ClO$_4$]$_2$ [X = Cl, Br; dppam = bis(diphenylphosphino)amine], derived from reaction

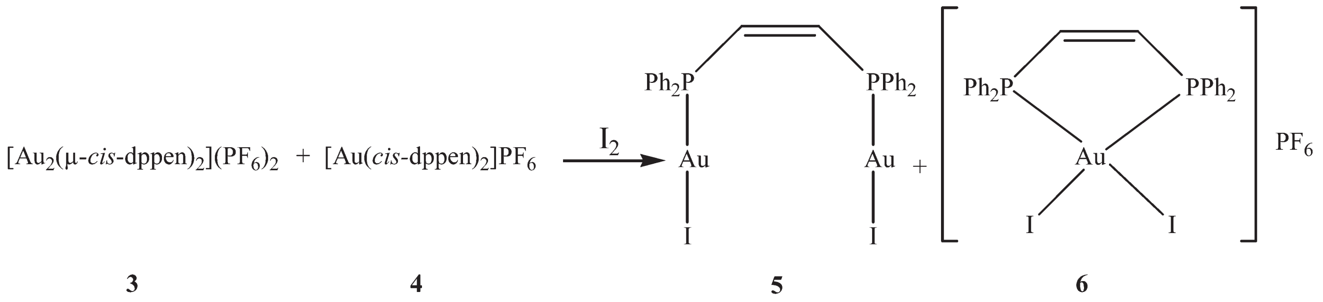

Scheme 2 Reaction of mixture of **3** and **4** with iodine.

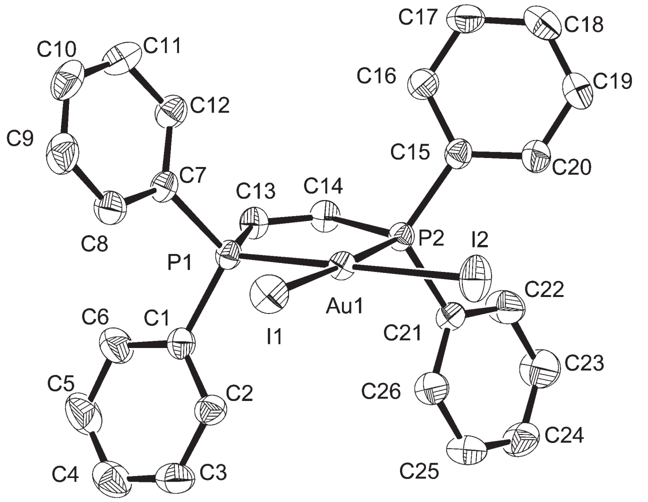

Fig. 2 The molecular structure of $[AuI_2(cis\text{-}dppen)]PF_6$ (**6**). Ellipsoids show 30% probability levels. Hydrogen atoms and PF_6 counterion have been omitted for clarity. Selected bond lengths (Å) and angles (°): Au(1)–P(1) 2.3189(12), Au(1)–P(2) 2.3273(12), Au(1)–I(1) 2.6306(4), Au(1)–I(2) 2.6246(4); P(1)–Au(1)–I(1) 90.84(3), P(2)–Au(1)–I(2) 89.36(3), P(1)–Au(1)–P(2) 86.60(4), I(1)–Au(1)–I(2) 93.218(15).

of $[Au_2(dppam)_2][ClO_4]_2$ with halogens.[41] Given the structural similarity between this gold(I) complex and $[Au_2(cis\text{-}dppen)_2](PF_6)_2$ (**3**), the oxidative addition reaction of halogens was investigated.

Treating a mixture of $[Au_2(cis\text{-}dppen)_2](PF_6)_2$ (**3**) and $[Au(cis\text{-}dppen)_2]PF_6$ (**4**) with I_2, Br_2 or $PhICl_2$ gave air- and moisture-stable red, yellow and pale yellow solids, respectively, whose ^{31}P NMR spectra showed two peaks [X = I (δ 15.6, 22.5), Br (δ 14.1, 22.6)] or four peaks [X = Cl (δ 10.1, 12.9, 21.1, 22.5)]. Recrystallization of the red powder (X = I) from dichloromethane/ether at −18 °C gave a mixture of colorless and red crystals, the identities of which were confirmed by X-ray crystallography study to be $[Au_2I_2(cis\text{-}dppen)]$ (**5**) and mononuclear gold(III) complex $[AuI_2(cis\text{-}dppen)]PF_6$ (**6**), respectively (Scheme 2). The crystal structures of $[Au_2I_2(cis\text{-}dppen)]$ (**5**) has been reported in literature and its photochemical conversion has been investigated.[42] By analogy to the observed trend in ^{31}P NMR resonances of $[(AuCl)_2(cis\text{-}dppen)]$ (δ 12.5) and $[Au(cis\text{-}dppen)_2]Cl$ (δ 22.4) in which dppen acts as bridging and chelating ligands, respectively, the resonance at δ 15.6 was assigned to **5** and the resonance at δ 22.5 to **6**.[43]

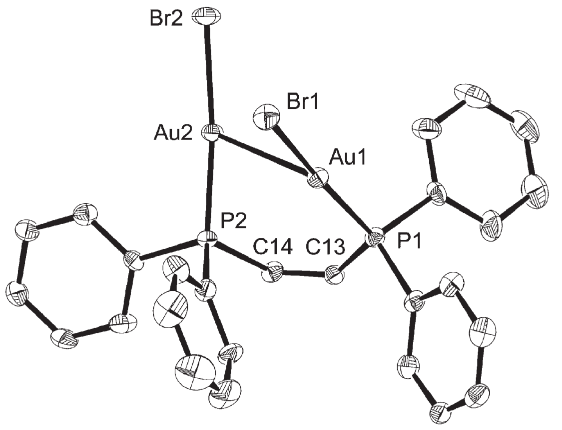

Fig. 3 Molecular structure of $[Au_2Br_2(cis\text{-}dppen)]$ (**7**). Ellipsoids show 50% probability levels. Hydrogen atoms have been omitted for clarity.

Table 1 Selected bond distances (Å) and angles (°) in complexes **5**, **7** and **9**

	5 (X = I)[a]	**5** (X = I)	**7** (X = Br)	**9** (X = Cl)[b]
Au(1)–Au(2)	2.9526(5)	2.9714(12)	3.0020(4)	3.05(1)
Au(1)–P(1)	2.256(3)	2.243(5)	2.2065(19)	2.226(4)
Au(2)–P(2)	2.253(2)	2.231(5)	2.2308(18)	2.239(5)
Au(1)–X(1)	2.5629(9)	2.5656(15)	2.4246(8)	2.299(5)
Au(2)–X(2)	2.5385(9)	2.5801(16)	2.4149(8)	2.289(5)
C(13)–C(14)	1.332(14)	1.30(3)	1.328(10)	1.331(18)
X(1)–Au(1)–P(1)	174.80(7)	171.44(14)	171.55(6)	172.5(2)
X(2)–Au(2)–P(2)	170.36(7)	169.37(14)	171.90(5)	173.3(2)

[a] Data from ref. 42. [b] Data from ref. 44.

Complex **6**, whose structure is shown in Fig. 2 (selected bond distances and angles of **6** are shown in the caption), consists of one gold(III) atom coordinated in a planar geometry by two mutually *cis* phosphorus atoms of a dppen ligand and two iodine atoms. The Au–P [2.323 (av.) Å] and Au–I [2.628 (av.) Å] distances are similar to the corresponding bonds in $[IAu(\mu\text{-}2\text{-}C_6H_3\text{-}6\text{-}Me\text{-}2\text{-}PPh_2)(\kappa^2\text{-}C_6H_3\text{-}6\text{-}Me\text{-}2\text{-}PPh_2)AuI]$ are 2.347(3) and 2.645(1) Å, respectively.[38]

Analogous reaction with Br_2 has formed two species which were tentatively assigned to complexes $[Au_2Br_2(cis\text{-}dppen)]$ (**7**) and $[AuBr_2(cis\text{-}dppen)]PF_6$ (**8**), based on their similar ^{31}P NMR chemical shifts (δ 14.1 and 22.6, respectively) to **5** and **6**. The structure of **7** was later confirmed by X-ray crystal structure

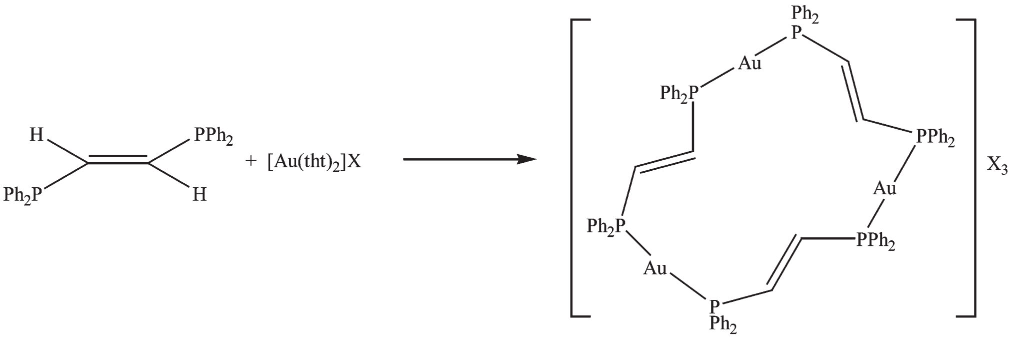

X = OTf **11**, PF_6 **12**

Scheme 3 Reaction of $[Au(tht)_2]X$ (X = OTf, PF_6) with one equivalent of *trans*-dppen.

determination and is shown in Fig. 3; selected bond distances in **7** are summarized in Table 1.

Reaction of the mixture of **3** and **4** with $PhICl_2$ was more complex than expected, and the resulting solid exhibited four ^{31}P NMR resonances, two of which at δ 12.9 and 22.5 can be assigned to $[Au_2Cl_2(cis\text{-dppen})]$ (**9**) $[AuCl_2(cis\text{-dppen})]PF_6$ (**10**), respectively, but the other two remain unidentified. Attempts to separate the pale yellow mixture (X = Cl) into its components by fractional crystallization from dichloromethane/ether at room temperature and at −18 °C were not successful.

The Au–Au distances in **5**, **7** and **9** decrease in the order Cl > Br > I. The gold(I) atoms in **5**, **7** and **9** are coordinated almost linearly by the phosphine and halogen atoms [∠X–Au–P *ca.* 170°]. The X–Au–P angle increases in the order I < Br < Cl, presumably due to the increasing size of halide.

Cyclic tri- and tetranuclear gold complexes

The reaction of $[Au(tht)_2]X$ (X = OTf, PF_6) with one equivalent of *trans*-dppen gave the cyclic trinuclear gold complexes $[Au_3(\mu\text{-}trans\text{-dppen})_3]X_3$ (X = OTf **11**, PF_6 **12**) (Scheme 3), as white powders in high yields. The ^{31}P NMR spectra of **11** and **12** each showed a single resonance at δ 41 ppm and the FAB mass spectra showed a peak at *m*/*z* 594. Elemental analyses were consistent with the empirical formula [Au(dppen)]X. The structure of **11** has been confirmed by single crystal X-ray diffraction (Fig. 4) and shown to be an energetic minimum by *ab initio* calculations. A comparison of selected bond lengths and angles is shown in Table 2. To aid in obtaining a chemically intuitive understanding of the structure, the charge state of the Au atoms was also calculated, and found to be neutral. Analysis of the electronic density of states showed a bandgap in the meV range, well under the onset of the visible spectrum near 1.77 eV.

The cyclic trication is generated by a crystallographic three-fold axis, and thus has a three-fold symmetric structure. Two of the three corresponding triflate ions are located on three-fold axes, surrounded with phenyl groups; the third triflate anion was heavily disordered and could not be located. Almost all of the known cyclic trinuclear gold(I) complexes reported in the literature contain bidentate N,N or C,N donor ligands; examples include $[Au_3(CH_3N{=}COCH_3)_3]$ **A**,[45] $[Au_3(pz)_3]$ (pz = 3,5-diphenylpyrazolato anion) **B**[46] and $[Au_3(NC_5H_4)_3]$ **C**.[47] The only reported cyclic trinuclear gold(I) complex containing a diphosphine ligand is $[Au_3(PAnP)_3](ClO_4)_3$ [PAnP = 9,10-bis(diphenylphosphino)anthracene].[48] While the conformations of the neutral complexes **A**, **B** and **C** are planar, those of **11** and $[Au_3(PAnP)_3](ClO_4)_3$ have a cyclohexane-like chair conformation. The Au–P distances in **11** [2.2923(11) and 2.3054(11) Å] are similar to those in **1** [2.2937(6) and 2.3172(6) Å] and $[Au_3(PAnP)_3](ClO_4)_3$ [2.294(3)–2.312(3) Å]. The gold atoms are almost linearly coordinated by two phosphorus atoms [P(1)–Au(1)–P(2) 174.20(4)°].

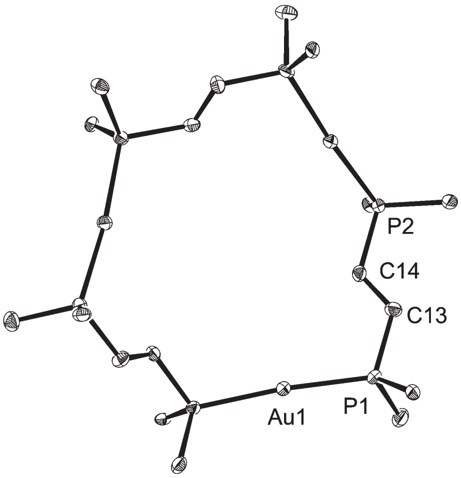

Fig. 4 Molecular structure of $[Au_3(\mu\text{-}trans\text{-dppen})_3](OTf)_3$ **11**. Ellipsoids show 30% probability levels. OTf counterions have been omitted for clarity and only the *ipso* carbons of the PPh_2 groups are shown.

Table 2 Selected bond distances (Å) and angles (°) in complex **11**

	XRD	DFT
Au(1)–P(1)	2.2923(11)	2.30
Au(1)–P(2)	2.3054(11)	2.30
P(1)–C(13)	1.786(4)	1.77
P(2)–C(14)	1.816(4)	1.77
P(1)–Au(1)–P(2)	174.20(4)	176.53
C(13)–P(1)–Au(1)	113.64(16)	114.25
C(14)–P(2)–Au(1)	112.83(14)	113.17

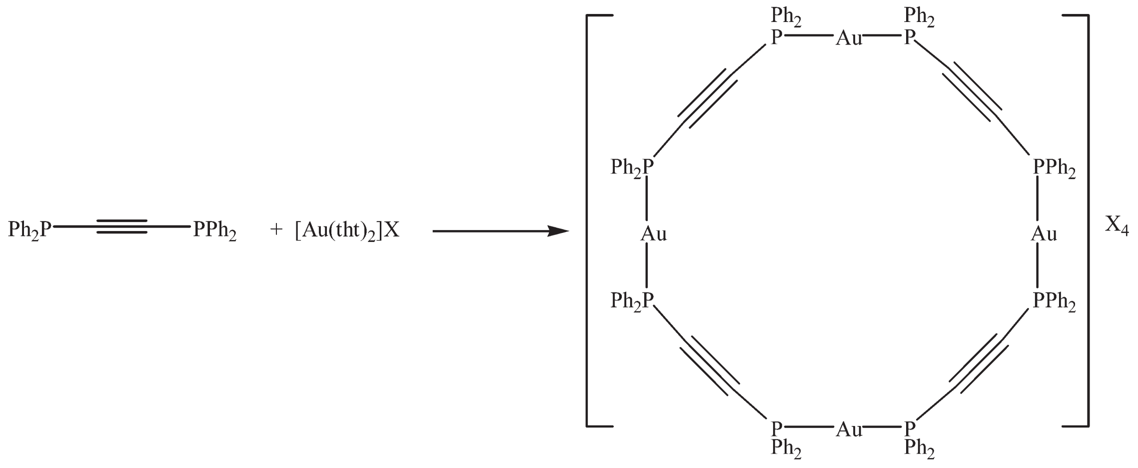

X = OTf **13**, PF$_6$ **14**, ClO$_4$ **15**

Scheme 4 Reaction of [Au(tht)$_2$]X with an equimolar amount of dppa.

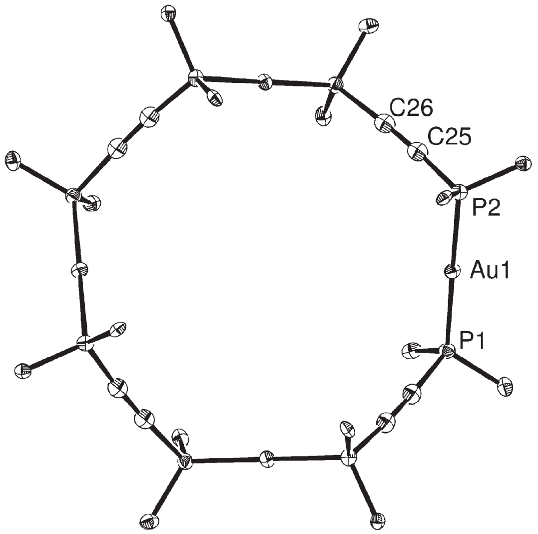

Fig. 5 Molecular structure of [Au$_4$(μ-dppa)$_4$](PF$_6$)$_4$ **14**. Ellipsoids show 20% probability levels. Only the *ipso* carbons of the PPh$_2$ groups are shown.

Table 3 Selected bond distances (Å) and angles (°) in complex **14**

	XRD	DFT
Au(1)–P(1)	2.278(2)	2.28
Au(1)–P(2)	2.295(2)	2.27
P(2)–C(25)	1.698(9)	1.73
C(25)–C(26)	1.239(16)	1.23
P(1)–Au(1)–P(2)	177.85(7)	177.67
C(25)–P(2)–Au(1)	114.2(5)	105.86
C(26)–C(25)–P(2)	175.3(16)	169.46

Tetranuclear gold(I) complexes [Au$_4$(μ-dppa)$_4$]X$_4$ (X = OTf **13**, PF$_6$ **14**, ClO$_4$ **15**), shown in Scheme 4, were prepared from the reaction of [Au(tht)$_2$]X with an equimolar amount of dppa. Complexes **13–15** each show a singlet at *ca.* δ 17 ppm in their ^{31}P NMR spectra and a parent ion peak in their FAB mass spectra. The structure of **14**, shown in Fig. 5, has been confirmed by X-ray crystallography from crystals grown from CH$_2$Cl$_2$/ether.

The XRD structure of [Au$_4$(μ-dppa)$_4$](PF$_6$)$_4$ **14** was of poor quality, and only used for confirming the overall structure. Several complexes containing Au$_4$L$_4$ type structure have been reported in the literature including P-bridged [{Au(PMes$_2$)}$_4$] (Mes = 2,4,6-Me$_3$C$_6$H$_2$),[49] N-bridged [{Au(μ-3,5-^{t}Bu-pz)}$_4$] (pz = pyrazolato anion),[50] [{Au[μ-N(SiMe$_3$)$_2$]}$_4$][51] and S-bridged [{Au$_2$(C$_6$H$_4$S$_2$-1,2)(PEt$_3$)}$_2$].[52] The XRD data for **14** was used to build a stable *ab initio* model without the structural disorder seen in the anions and phenyl groups; a comparison of selected bond lengths (Å) and angles (°) is shown in Table 3. Analysis of the electronic density of states showed a bandgap in the meV range (~80 meV), with energies far less than those of photons in the visible spectrum. The charge state of the Au atoms was evaluated as neutral.

Interestingly, recrystallization of **15** from CH$_2$Cl$_2$/MeOH gave orange crystals which were shown by X-ray crystallography to be the octanuclear gold cluster [Au$_8$Cl$_2$(μ-dppa)$_4$](ClO$_4$)$_2$ **16**; all attempts to isolate **16** in a pure form failed. The structure of **16** is shown in Fig. 6 and selected bond lengths and angles are summarized in Tables 4 and 5, respectively. This structure has been modeled with *ab initio* techniques, and analysis of the electronic density of states gave a bandgap of 2.05 eV, corresponding to a photon of wavelength 605 nm which matches well with the observation of orange (~590 nm) crystals.

The complex **16** has −1 symmetry and contains eight gold atoms, six of which form two edge-shared tetrahedra with Au–Au distances in the range of 2.6–2.8 Å. Coordinated to the two gold atoms of the Au$_6$ core, sitting in the vertices of the shared edges of two tetrahedra, are two dppa ligands, which also coordinate from the other side to the terminal univalent gold atoms, bonded to chlorine groups and phosphorus atoms of bridging bis(diphenylphosphino)acetylene; these gold atoms exhibit linear

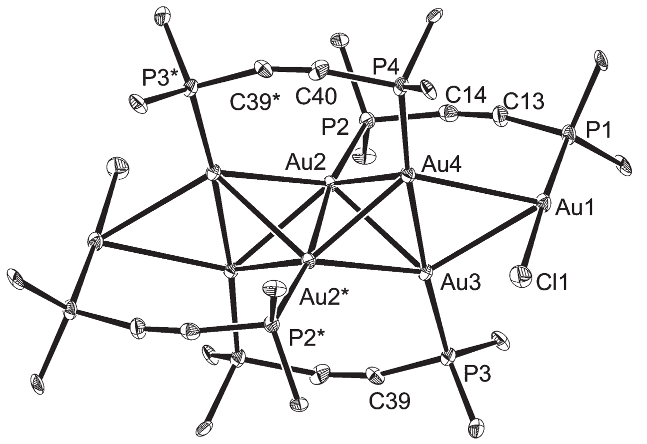

Fig. 6 Molecular structure of **16**. Ellipsoids show 50% probability levels. The phenyl rings of the PPh_2 groups only show the *ipso* carbons. Atoms with an * in the atom labels are at equivalent position (2 − *x*, 1 − *y*, −*z*) generated by inversion symmetry.

Table 4 Selected bond lengths (Å) in **16**

Bond	XRD	DFT	Bond	XRD	DFT
Au(1)–Au(4)	2.9738(6)	3.06	—	—	—
Au(2)–Au(4)	2.8144(6)	2.89	Au(3)–Au(2)	2.8403(5)	2.87
Au(3)–Au(4)	2.6205(6)	2.67	Au(1)–P(1)	2.245(3)	2.28
Au(1)–Au(3)	3.0522(6)	3.00	Au(2)–P(2)	2.276(2)	2.31
Au(2)–Au(2*)	2.6192(7)	2.69	Au(3)–P(3)	2.297(3)	2.32
Au(2)–Au(3*)	2.7887(5)	2.85	Au(4)–P(4)	2.294(3)	2.32
Au(2)–Au(4*)	2.7989(6)	2.83	Au(1)–Cl(1)	2.313(2)	2.35

Asterisks denote atoms generated by symmetry.

coordination (*ca.* 177°). The other four gold atoms in the Au_6 core are coordinated by two dppa ligands to generate a 12-membered ring in which the gold atoms display almost linear geometry (*ca.* 175°). The structure is comprised of the twelve-membered ring and an S-shaped chain; the two fragments are held together by aurophilic interactions. The shortest gold–gold distances in **16** are between Au(2) and Au(2*) [2.6192(7) Å] and Au(3) and Au(4) [2.6205(6) Å], slightly shorter than those reported for the Au_5 cluster $[Au_5(C_6H_4PPh_2)_4]CF_3SO_3$ (**2**-OTf) [2.709(2) and 2.701(2) Å] obtained by the reaction of $[Au_2(C_6H_4PPh_2)_2]$ with trifluoromethanesulfonate at −78 °C.[53] The gold–gold distances in **16** [*ca.* 2.6–3 Å] are typical of gold–phosphine clusters, $[Au_8(PPh_3)_8](aliz)_2$ (aliz = alizarinsulphonate) [2.587(5)–2.878 Å],[54] $[Au_8(PPh_3)_8](PF_6)_2]$ [2.635(8)–2.896(8) Å],[55] $[Au_5(dppmH)_3(dppm)](NO_3)_2$ [dppm = $(Ph_2PCHPPh_2)^-$] (2.70–3.01 Å),[56] $[Au_9\{P(C_6H_4\text{-}p\text{-}Me)_3\}_8](PF_6)_3$ 2.689(3)–2.868(3) Å,[57] and $[Au_8(PPh_3)_7](NO_3)_2$ [2.629(5)–2.942(6) Å].[58]

Photophysical studies

The electronic absorption data of the cyclic gold(I) complexes $[Au_3(\mu\text{-}trans\text{-dppen})_3]X_3$ (X = OTf **11**, PF_6 **12**) and $[Au_4(\mu\text{-dppa})_4]X_4$ (X = OTf **13**, PF_6 **14**) in dichloromethane at

Table 6 Electronic absorption data for complexes **11–14** in dichloromethane at ambient temperature

Compound	λ_{abs}/nm (ε/dm^3 mol^{-1} cm^{-1})
11	268 sh (34 505), 278 sh (24 245)
12	268 sh (33 595), 278 sh (23 710)
13	272 sh (27 740), 278 sh (22 070)
14	272 sh (26 190), 280 sh (18 200)

Table 5 Selected bond angles (°) in **16**

Bond angle	XRD	DFT	Bond angle	XRD	DFT
Au(2*)–Au(2)–Au(3)	61.275(16)	61.54	Au(2)–Au(4)–Au(1)	112.874(17)	108.78
Au(2*)–Au(2)–Au(3*)	63.274(16)	62.37	Au(2*)–Au(4)–Au(1)	124.594(17)	122.36
Au(2*)–Au(2)–Au(4)	61.886(16)	60.92	Au(2*)–Au(4)–Au(2)	55.627(16)	55.95
Au(2*)–Au(2)–Au(4*)	62.487(17)	63.14	Au(3*)–Au(2)–Au(3)	124.549(15)	123.91
Au(2)–Au(3)–Au(1)	109.853(16)	111.15	Au(3*)–Au(2)–Au(4*)	55.938(13)	56.14
Au(2*)–Au(3)–Au(1)	122.060(17)	124.12	Au(3*)–Au(2)–Au(4)	97.959(17)	96.61
Au(2*)–Au(3)–Au(2)	55.451(15)	56.09	Au(3)–Au(4)–Au(1)	65.776(15)	62.70
Au(3)–Au(4)–Au(2*)	61.834(14)	62.16	Au(4)–Au(2)–Au(3)	55.215(14)	55.28
Au(3)–Au(4)–Au(2)	62.893(14)	61.89	Au(4*)–Au(2)–Au(3)	97.118(16)	97.45
Au(4)–Au(1)–Au(3)	51.535(13)	52.27	Au(4*)–Au(2)–Au(4)	124.373(16)	124.05
Au(4)–Au(3)–Au(1)	62.689(14)	65.02	Cl(1)–Au(1)–Au(3)	74.92(7)	79.54
Au(4)–Au(3)–Au(2)	61.891(14)	62.83	Cl(1)–Au(1)–Au(4)	78.68(7)	74.88
Au(4)–Au(3)–Au(2*)	62.228(14)	61.70	P(1)–Au(1)–Au(3)	105.71(7)	104.33
P(1)–Au(1)–Au(4)	103.83(7)	106.76	P(1)–Au(1)–Cl(1)	177.26(10)	176.05
P(2)–Au(2)–Au(2*)	170.11(7)	170.23	P(2)–Au(2)–Au(3)	109.47(7)	111.12
P(2)–Au(2)–Au(3*)	125.86(7)	124.55	P(2)–Au(2)–Au(4)	110.60(7)	109.91
P(2)–Au(2)–Au(4*)	124.61(7)	125.93	P(3)–Au(3)–Au(1)	113.33(7)	111.34
P(3)–Au(3)–Au(2)	120.95(7)	118.07	P(3)–Au(3)–Au(2*)	121.50(7)	122.37
P(3)–Au(3)–Au(4)	176.02(7)	175.83	P(4)–Au(4)–Au(1)	109.75(7)	113.96
P(4)–Au(4)–Au(2)	118.96(7)	120.07	P(4)–Au(4)–Au(2*)	122.95(7)	121.14
P(4)–Au(4)–Au(3)	175.21(7)	176.64	—	—	—

Asterisks denote atoms generated by symmetry.

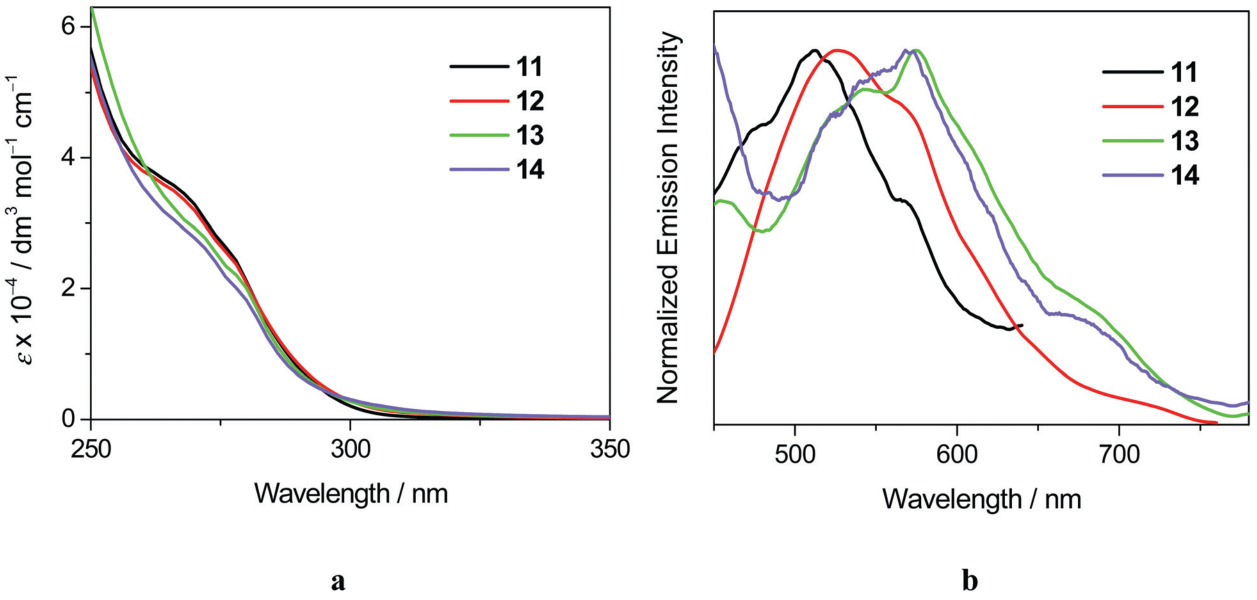

Fig. 7 (a) Electronic absorption spectra of complexes **11–14** in dichloromethane at ambient temperature; (b) normalized emission spectra of complexes **11–14** in butyronitrile glass at 77 K.

ambient temperature are summarized in Table 6 and the absorption spectra are shown in Fig. 7a. All complexes display spin-allowed intraligand ^{1}IL and metal-perturbed intraligand ^{1}IL shoulders at 268–280 nm.[59–61] The complexes are non-emissive at room temperature. Upon photo-excitation in butyronitrile glass at 77 K, the complexes reveal weak emission (Fig. 7b).

With reference to the previous reports on the photophysical studies of gold(I)–phosphine complexes,[59–61] the high-energy emission bands are tentatively assigned to originate from spin-forbidden metal-perturbed intraligand ^{3}IL (phosphine) exited states. The slightly higher emission energy of **11** and **12** than **13** and **14** is consistent with the higher intraligand (phosphine) exited state energy of $Ph_2PCH{=}CHPPh_2$ than the more conjugated $Ph_2PC{\equiv}CPPh_2$. The lack of emissive properties at room temperature is probably due to the floppy nature of the metallamacrocyclic ring structure of the complexes.

Given the structural similarities between $[Au_2(\mu\text{-}cis\text{-dppen})_2]X$- ($X$ = OTf **1**, PF_6 **3**) and previously reported luminescent gold complexes,[62] one would expect these compounds to be prospective candidate for photophysical study. The initial investigation was carried out by exposing the mixtures of $[Au_2(\mu\text{-}cis\text{-dppen})_2]X$ (X = OTf **1**, PF_6 **3**) and $[Au(cis\text{-dppen})_2]X$ (X = OTf **2**, PF_6 **4**) to UV radiation. As the mixtures did not appear to be luminescent under UV light at room temperature, and several attempts to separate the components of mixtures were failed, this was not pursued further.

Conclusion

Diphosphine ligands have been used to prepare mono, di, tri and tetranuclear cyclic complexes. The reaction of *cis*-dppen with $[Au(tht)_2]X$ failed to give a pure product, but rather a mixture of $[Au_2(\mu\text{-}cis\text{-dppen})_2]X$ (X = OTf_2 **1**, PF_6 **3**) and $[Au(cis\text{-dppen})_2]$ X (X = OTf **2**, PF_6 **4**). The mixture of **3** and **4** reacted with halogens to give a mixture of acyclic binuclear gold(I) $[Au_2X_2$ (*cis*-dppen)] (X = I **5**, Br **7**, Cl **9**) and cyclic mononuclear gold(III) complex $[AuX_2(cis\text{-dppen})]PF_6$ (X = I **6**, Br **8**, Cl **10**). In contrast to the *cis*-isomer, the reaction of *trans*-dppen with $[Au(tht)_2]X$ gives the cyclic trinuclear complexes $[Au_3(\mu\text{-}trans\text{-dppen})_3]X_3$ (X = OTf **11**, PF_6 **12**). Effect of geometry of ligand has been shown to be an important factor in the reaction of dppen with tetrachloroaurate.[31] When dppa used, reaction proceeded in a different direction to give high nuclearity species, tetranuclear gold complexes $[Au_4(\mu\text{-dppa})_4]X_4$ (X = OTf **13**, PF_6 **14**, ClO_4 **15**); recrystallization of the last of three from CH_2Cl_2/MeOH gave orange crystals which proved to be an octanuclear gold cluster by X-ray crystallography.

Experimental section

General comments

^{1}H NMR and ^{31}P NMR spectra were recorded on a JEOL JNM-ECP 400 or Varian Gemini 300 NMR spectrometer as $CDCl_3$ solutions, referenced to residual solvent peaks; ^{31}P NMR spectra were obtained as proton-decoupled. FAB-mass spectra were measured on a JEOL JMS-600H spectrometer in positive ion mode. Elemental analyses were carried out in-house on a Perkin-Elmer 2400 analyzer or at the Microanalytical Laboratory of the Research School of Chemistry, Australian National University. Crystals suitable for single-crystal X-ray diffraction were obtained by layering a dichloromethane solution of the complex with hexane.

X-ray crystallography

All diffraction data were collected on a Bruker SMART CCD area detector diffractometer with graphite monochromated Mo-Kα radiation (λ = 0.71073 Å). Geometric and intensity data were collected using SMART software.[63] The data were processed using SAINT,[64] and corrections for absorption were applied using

Table 7 Crystal data and details of data collection and structure refinement for complexes **1**, **5–7**, **11**, **14** and **16**

Compound	**1**	**5**	**6**	**7**
Formula	$C_{54}H_{44}Au_2F_6O_6P_4S_2$	$C_{26}H_{22}Au_2I_2P_2$	$C_{26}H_{22}AuF_6I_2P_3$	$C_{26}H_{22}Au_2Br_2P_2$
FW	1484.82	1044.12	992.11	950.12
Crystal system	Triclinic	Monoclinic	Monoclinic	Monoclinic
Space group	$P\bar{1}$	Cc	$P2(1)/c$	Cc
a (Å), b (Å), c (Å)	10.8043(6), 10.9164(6), 11.7847(6)	13.340(4), 12.988(4), 16.396(5)	17.6151(8), 9.3424(4), 19.5736(9)	13.2194(7), 12.9069(7), 15.6042(8)
α (°), β (°), γ (°)	76.473(1), 82.956(1), 73.340(1)	90, 103.629(6), 90	90, 111.3970(10), 90	90, 101.7360(10), 90
V (Å^3)	1292.35(12)	2760.9(14)	2999.2(2)	2606.8(2)
Z	1	4	4	4
D_{calc} (mg m^{-3})	1.908	2.512	2.197	2.421
μ (mm^{-1})	5.947	12.980	7.177	14.444
T (K)	90(2)	173(2)	298(2)	173(2)
Crystal dimensions (mm)	0.46 × 0.22 × 0.14	0.30 × 0.098 × 0.093	0.28 × 0.096 × 0.064	0.36 × 0.26 × 0.22
θ range (°)	1.78–28.30	2.22–28.30	2.24–28.34	2.23–28.31
Reflections collected	9611	9041	21 835	9391
Unique (R_{int}) [χ Flack]	6330 (0.0179)	4731 (0.0496) [0.00(1)]	7463 (0.0251)	4834 (0.0249) [0.00(1)]
Data/restrains/parameters	6330/0/334	4731/2/289	7463/0/343	4834/2/289
Final R indices [$I > 2\sigma(I)$]	$R1 = 0.0217$, w$R2 = 0.0583$	$R1 = 0.0554$, w$R2 = 0.1360$	$R1 = 0.0338$, w$R2 = 0.0889$	$R1 = 0.0259$, w$R2 = 0.0624$
R indices (all data)	$R1 = 0.0221$, w$R2 = 0.0586$	$R1 = 0.0651$, w$R2 = 0.1427$	$R1 = 0.0425$, w$R2 = 0.0942$	$R1 = 0.0265$, w$R2 = 0.0626$
Largest diff. peak and hole (e Å^{-3})	1.881 and −2.224	3.867 and −4.442	1.621 and −1.270	1.229 and −1.005

Compound	**11**	**14**	**16**
Formula	$C_{88}H_{80}Au_3Cl_{14}F_9O_9P_6S_3$	$C_{108.50}H_{89}Au_4Cl_9F_{24}P_{12}$	$C_{106}H_{82}Au_8Cl_{10}O_8P_8$
FW	2821.71	3327.35	3661.71
Crystal system	Trigonal	Tetragonal	Triclinic
Space group	$R3c$	$P4/ncc$	$P\bar{1}$
a (Å), b (Å), c (Å)	19.9108(2), 19.9108(2), 39.4563(7)	19.2584(2), 19.2584(2), 32.3309(5)	12.6200(11), 13.6183(11), 16.8190(14)
α (°), β (°), γ (°)	90, 90, 120	90, 90, 90	72.088(2), 73.716(2), 82.431(2)
V (Å^3)	13 546.4(3)	11 991.1(3)	2636.8(4)
Z	6	4	1
D_{calc} (mg m^{-3})	2.075	1.843	2.306
μ (mm^{-1})	5.531	5.323	11.513
T (K)	100(2)	150(2)	90(2)
Crystal dimensions (mm)	0.25 × 0.18 × 0.12	0.22 × 0.18 × 0.12	0.16 × 0.063 × 0.044
θ range (°)	2.57–28.00	1.96–25.00	1.57–28.34
Reflections collected	77 102	49 276	19 687
Unique (R_{int}) [χ Flack]	7265(0.0555) [0.00(8)]	5283(0.0542)	12 955(0.0395)
Data/restrains/parameters	7265/1/311	5283/13/275	12 955/0/631
Final R indices [$I > 2\sigma(I)$]	$R1 = 0.0256$, w$R2 = 0.0618$	$R1 = 0.0468$, w$R2 = 0.1484$	$R1 = 0.0555$, w$R2 = 0.1194$
R indices (all data)	$R1 = 0.0276$, w$R2 = 0.0626$	$R1 = 0.0703$, w$R2 = 0.1586$	$R1 = 0.0783$, w$R2 = 0.1291$
Largest diff. peak and hole (e Å^{-3})	0.730 and −0.401	1.289 and −1.250	4.114 and −1.551

SADABS.[65] The data sets of **1**, **6**, **7**, **10**, **11** were further treated with an Xabs2 absorption correction as implemented in WinGX.[66] All structures were solved by direct methods using the SHELX-TL package.[67] Crystallographic data are summarized in Table 7. The structure of **13** contains heavily disordered anions and solvent molecules. After an initial refinement, which revealed three sites in the asymmetric unit accessible to solvent molecules, the data set was treated with SQUEEZE as implemented in WinGX PLATON.[68] CCDC reference numbers 843620–843626 refer to the crystals structures reported in this paper.

Computational details

Ab initio calculations were performed using the Vienna *ab initio* simulation package (VASP) developed at the Universität Wien.[69] Calculations were performed using the PBE GGA correlation-exchange functional,[70] and projector augmented-wave (PAW)[71] potentials for all atoms. The plane-wave cutoff was set at 400 eV for all calculations. A 2 × 2 × 2 Monkhorst-Pack *k*-point mesh was used. All calculations were performed by constructing a supercell from the XRD data. For compound **14**, some atoms with fractional occupancies in the XRD data were omitted (though their counterparts were retained). In performing the geometry optimization, relaxation was alternately applied to the ionic coordinates and the cell parameters, before allowing both to vary. Final stresses on the supercell were less than 3 kB in magnitude. Charge analysis was performed using the Bader method,[72] as implemented in ref. 73–75. Bandgap comparisons were performed in the manner of Chilukuri and Cundari,[76] who used the HOMO–LUMO gap derived from the electronic density of states (eDOS) as a fundamental predictor of several effects.

Due to the size of the primitive cells (several hundred atoms), this is currently the limit to which theory can be used to predict optical properties of these crystals. Techniques such as time-dependent density functional theory, which also take account of the excited states of systems, are simply not computationally tractable in these cases.

Photophysical measurements and instrumentation

The electronic absorption spectra were recorded on a Hewlett-Packard 8452A diode array spectrophotometer. Steady-state emission spectra recorded at room temperature and at 77 K were measured on a Spex Fluorolog-3 Model FL3-211 fluorescence spectrofluorometer equipped with a R2658P PMT detector. Low-temperature butyronitrile glass photophysical measurements were carried out with the sample in a quartz tube inside a quartz-walled Dewar flask with liquid nitrogen.

Syntheses

$[Au_2(\mu$-*cis*-dppen$)_2]X_2$ (X = OTf 1, PF_6 3) and $[Au($*cis*-dppen$)_2]X$ (X = OTf 2, PF_6 4). To a stirred solution of $[Au(tht)_2]X$ (X = OTf, PF_6) (0.334 mmol) in dichloromethane (30 mL) was added an equimolar amount of *cis*-dppen (0.334 mmol) at room temperature. The mixture was stirred for 30 min and then was filtered through Celite. The volume of the solution was reduced to half under reduced pressure and ether was added, precipitating out the product.

^1H NMR($CDCl_3$): δ 7.09–7.58 (m, aromatics). ^{31}P NMR ($CDCl_3$): δ 23.1, 25.1. FAB-MS (*m/z*): 1338 $[Au_2(dppen)_2OTf + H]^+$, 1334 $[Au_2(dppen)_2PF_6 + H]^+$, 1187 $[Au_2(dppen)_2 + H]^+$.

$[Au_2I_2($*cis*-dppen$)]PF_6$ (X = I 5, Br 7, Cl 9) and $[AuI_2($*cis*-dppen$)]PF_6$ (X = I 6, Br 8, Cl 10). A mixture of **3** and **4** (50 mg, 0.04 mmol) in dichloromethane (10 mL) was treated with a solution of $PhICl_2$, bromine or iodine (0.04 mmol) in dichloromethane at room temperature. The suspension was shielded from light and stirred for 1 h. The solvent was removed under reduced pressure and ether was added to give a precipitate which was isolated by filtration, washed with ether and dried.

With $PhICl_2$: Yield 40 mg, ^{31}P NMR ($CDCl_3$): δ 10.1, 12.9, 21.1, 22.5. FAB-MS (*m/z*): 827, 1241, 1023, 991.

With bromine: Yield 36 mg, ^{31}P NMR ($CDCl_3$): δ 14.1, 22.6. FAB-MS (*m/z*): 873, 992.

With iodine: Yield 47 mg, ^{31}P NMR ($CDCl_3$): δ 15.6, 22.5. FAB-MS (*m/z*): 991, 914, 764.

$[Au_3(\mu$-*trans*-dppen$)_3]X_3$ (X = OTf 11, PF_6 12). To a stirred solution of $[Au(tht)_2]X$ (X = OTf, PF_6) (0.334 mmol) in dichloromethane (30 mL) was added an equimolar amount of *trans*-dppen (0.334 mmol) at room temperature. The mixture was stirred for 30 min and then was filtered through Celite. The volume of the solution was reduced to half under reduced pressure and ether was added, precipitating out the white product.

11 Yield: 229 mg, 93%. ^1H NMR ($CDCl_3$): δ 7.05–7.73 (m, aromatics). ^{31}P NMR ($CDCl_3$): δ 41.6. FAB-MS (*m/z*): 594 $[Au_3(dppen)_3]^{+3}$, Anal. Calcd for $C_{78}H_{66}Au_3F_{18}P_9$: C 42.30, H 3.00. Found: C 41.73, H 2.86.

12: Yield: 196 mg, 79%. ^1H NMR ($CDCl_3$): δ 7.19–7.55 (m, aromatics). ^{31}P NMR ($CDCl_3$): δ 40.7. FAB-MS (*m/z*): 594 $[Au_3(dppen)_3]^{+3}$, Anal. Calcd for $C_{81}H_{66}Au_3F_9O_9P_6S_3$: C 43.68, H 2.99. Found: C 43.36, H 2.70.

$[Au_4(\mu\text{-dppa})_4]X_4$ (X = OTf 13, PF_6 14, ClO_4 15). In an analogous reaction to that described above, treatment of a dichloromethane solution of $[Au(tht)_2]X$ (X = OTf, PF_6, ClO_4) (0.34 mmol) with an equimolar amount of bis(diphenylphosphino)acetylene gave the title products.

13: Yield: 213 mg, 86%. ^1H NMR ($CDCl_3$): δ 7.19–7.80 (m, aromatics). ^{31}P NMR ($CDCl_3$): δ 17.0. FAB-MS (*m/z*): 592 $[Au_4(dppa)_4 + H]^{+4}$, Anal. Calcd for $C_{108}H_{80}Au_4F_{12}O_{12}P_8S_4$: C 43.80, H 2.72. Found: C 44.12, H 2.89.

14: Yield: 241 mg, 98%. ^1H NMR ($CDCl_3$): δ 7.13–7.73 (m, aromatics). ^{31}P NMR ($CDCl_3$): δ 17.1. FAB-MS (*m/z*): 592 $[Au_4(dppa)_4 + H]^{+4}$, Anal. Calcd for $C_{104}H_{80}Au_4F_{24}P_{12}$: C 42.41, H 2.74. Found: C 42.51, H 2.76.

15: Yield: 208 mg, 90%. ^1H NMR ($CDCl_3$): δ 7.16–7.79 (m, aromatics). ^{31}P NMR ($CDCl_3$): δ 18.3. FAB-MS (*m/z*): 592 $[Au_4(dppa)_4 + H]^{+4}$.

Acknowledgements

VWWY acknowledges support from the Areas of Excellence Scheme of the University Grants Committee of Hong Kong (AoE/P-03/08).

References

1 G. Schill, *Catenanes, Rotaxanes and Knots*, Academic Press, New York, 1971.
2 J. P. Sauvage and C. O. Dietrich-Buchecker, in *Molecular Catenanes, Rotaxanes and Knots*, ed. J. P. Sauvage and C. O. Dietrich-Buchecker, Wiley-VCH, Weinheim, 1999, pp. 57–75.
3 D. B. Amabilino and J. F. Stoddart, *Chem. Rev.*, 1995, **95**, 2725–2828.
4 J. C. Vickery, M. M. Olmstead, E. Y. Fung and A. L. Balch, *Angew. Chem., Int. Ed. Engl.*, 1997, **36**, 1179–1181.
5 C. P. McArdle, M. J. Irwin, M. C. Jennings and R. J. Puddephatt, *Angew. Chem., Int. Ed.*, 1999, **38**, 3376–3378.
6 C. P. McArdle, J. J. Vital and R. J. Puddephatt, *Angew. Chem., Int. Ed.*, 2000, **39**, 3819–3822.
7 R. J. Puddephatt, *Coord. Chem. Rev.*, 2001, **216–217**, 313–332.
8 J. H. K. Yip and J. Prabhavathy, *Angew. Chem., Int. Ed.*, 2001, **40**, 2159–2162.
9 F. Mohr, M. C. Jennings and R. J. Puddephatt, *Angew. Chem., Int. Ed.*, 2004, **43**, 969–971.
10 R. Lin, J. H. K. Yip, K. Zhang, L. L. Koh, K. Y. Wong and K. P. Ho, *J. Am. Chem. Soc.*, 2004, **126**, 15852–15869.
11 H. Schmidbaur, *Gold: Progress in Chemistry, Biochemistry and Technology*, Wiley, Chichester, 1999.
12 J. H. William, C. J. Michael and R. J. Puddephatt, *Z. Naturforsch.*, 2004, **59b**, 1488–1496.
13 M. C. Brandys, M. C. Jennings and R. J. Puddephatt, *J. Chem. Soc., Dalton Trans.*, 2000, 4601–4606.
14 (*a*) S.-Y. Yu, Z.-X. Zhang, E. C.-C. Cheng, Y.-Z. Li, V. W.-W. Yam, H.-P. Huang and R. Zhang, *J. Am. Chem. Soc.*, 2005, **127**, 17994–17995; (*b*) Q.-F. Sun, T. K.-M. Lee, P.-Z. Li, L.-Y. Yao, J.-J. Huang, J. Huang, S.-Y. Yu, Y.-Z. Li, E. C.-C. Cheng and V. W.-W. Yam, *Chem. Commun.*, 2008, 5514–5516; (*c*) S.-Y. Yu, Q.-F. Sun, T. K.-M. Lee, E. C.-C. Cheng, Y.-Z. Li and V. W.-W. Yam, *Angew. Chem., Int. Ed.*, 2008, **47**, 4551–4554.
15 G. A. Bowmaker, C. L. Brown, R. D. Hart, P. C. Healy, C. E. F. Rickard and A. H. White, *J. Chem. Soc., Dalton Trans.*, 1999, 881–890.
16 C. P. McArdle, S. Van, M. C. Jennings and R. J. Puddephatt, *J. Am. Chem. Soc.*, 2002, **124**, 3959–3965.

17 Z. Qin, M. C. Jennings and R. J. Puddephatt, *Chem.–Eur. J.*, 2002, **8**, 735–738.

18 H. Ehlich, A. Schier and H. Schmidbaur, *Inorg. Chem.*, 2002, **41**, 3721–3727.

19 J. P. Fackler Jr., *Inorg. Chem.*, 2002, **41**, 6959–6972.

20 F. Mendizabal, P. Pyykkö and N. Puneberg, *Chem. Phys. Lett.*, 2003, **370**, 733–740.

21 P. Schwerdtfeger, H. L. Hermann and H. Schmidbaur, *Inorg. Chem.*, 2003, **42**, 1334–1342.

22 A. Codina, E. J. Fernandez, P. G. Jones, A. Laguna, J. M. Lopez de Luzuriaga, M. Monge, M. E. Olmos, J. Perez and M. A. Rodriguez, *J. Am. Chem. Soc.*, 2002, **124**, 6781–6786.

23 L. J. Hao, M. A. Mansour, R. J. Lachicotte, H. J. Gysling and R. Eisenberg, *Inorg. Chem.*, 2000, **39**, 5520–5529.

24 C. P. McArdle, M. J. Irwin, M. C. Jennings and R. J. Puddephatt, *Angew. Chem., Int. Ed.*, 1999, **38**, 3376–3378.

25 C. E. Briant, K. P. Hall and D. M. P. Mingos, *J. Organomet. Chem.*, 1982, **229**, C5–C8.

26 H. Schmidbaur, A. Wohlleben, U. Schubert, A. Frank and G. Huttner, *Chem. Ber.*, 1977, **110**, 2751–2757.

27 R. M. Dávila, A. Elduque, T. Grant, R. J. Staples and J. P. Fackler Jr., *Inorg. Chem.*, 1993, **32**, 1749–1755.

28 R. M. Dávila, A. Elduque, R. J. Staples, M. Harlass and J. P. Fackler Jr., *Inorg. Chim. Acta*, 1994, **217**, 45–49.

29 C. E. Briant, K. P. Hall and D. M. P. Mingos, *J. Organomet. Chem.*, 1982, **229**, C5–C8.

30 S. J. Berners-Price, M. A. Mazid and P. J. Sadler, *J. Chem. Soc., Dalton Trans.*, 1984, 969–974.

31 C. A. McAuliffe, R. V. Parish and P. D. Randall, *J. Chem. Soc., Dalton Trans.*, 1979, 1730–1735.

32 A. Deák, T. Tunyogi, Z. Károly, S. Klébert and G. Pálinkás, *J. Am. Chem. Soc.*, 2010, **132**, 13627–13629.

33 C.-M. Che, H.-L. Kwong, V. W.-W. Yam and K.-C. Cho, *J. Chem. Soc., Chem. Commun.*, 1989, 885–886.

34 C.-M. Che, H.-K. Yip, W.-C. Lo and S.-M. Peng, *Polyhedron*, 1994, **13**, 887–890.

35 V. W.-W. Yam, T.-F. Lai and C.-M. Che, *J. Chem. Soc., Dalton Trans.*, 1990, 3747–3752.

36 S. J. Berners-Price, L. A. Colquhoun, P. C. Healy, K. A. Byriel and J. V. Hanna, *J. Chem. Soc., Dalton Trans.*, 1992, 3357–3363.

37 H. Schmidbaur, *Gold Bull.*, 1990, **23**, 11–21.

38 S. K. Bhargava, F. Mohr, M. A. Bennett, L. L. Welling and A. C. Willis, *Organometallics*, 2000, **19**, 5628–5635.

39 W. Schuh, H. Kopacka, K. Wurst and P. Peringer, *Chem. Commun.*, 2001, 2186–2187.

40 (*a*) H. Schmidbaur, *Gold: Progress in Chemistry, Biochemistry and Technology*, Wiley, Chichester, 1999; (*b*) A. Laguna and M. Laguna, *Coord. Chem. Rev.*, 1999, **193–195**, 837–856; (*c*) J. D. Basil, H. H. Murray, J. P. Fackler Jr., J. Tocher, A. M. Mazany, B. Trzcinska-Bancroft, H. Knachel, D. Dudis, T. J. Delord and D. O. Marler, *J. Am. Chem. Soc.*, 1985, **107**, 6908–6915; (*d*) M. N. I. Khan, J. P. Fackler Jr., C. King, J. C. Wang and S. Wang, *Inorg. Chem.*, 1988, **27**, 1672–1673; (*e*) H. H. Murray, J. P. Fackler Jr., L. C. Porter, D. A. Briggs, M. A. Guerra and R. J. Lagow, *Inorg. Chem.*, 1987, **26**, 357–363; (*f*) M. N. I. Khan, S. Wang and J. P. Fackler Jr., *Inorg. Chem.*, 1989, **28**, 3579–3588; (*g*) V. W.-W. Yam, S. W.-K. Choi and K.-K. Cheung, *Chem. Commun.*, 1996, 1173–1174; (*h*) V. W.-W. Yam, C.-K. Li, C.-L. Chan and Kung-Kai Cheung, *Inorg. Chem.*, 2001, **40**, 7054–7058; (*i*) M. A. Bennett, S. K. Bhargava, N. Mirzadeh, S. H. Privér, J. Wagler and A. C. Willis, *Dalton Trans.*, 2009, 7537–7551.

41 R. Usón, A. Laguna, M. Laguna and N. Fraile, *J. Chem. Soc., Dalton Trans.*, 1986, 291–296.

42 J. B. Floey, S. E. Gay, M. J. Vela, B. M. Foxman, A. E. Bruce and M. R. M. Bruce, *Eur. J. Inorg. Chem.*, 2007, 4946–4951.

43 D. S. Khanye, J. Caddy and M. Layh, *Gold Bull.*, 2007, **40** (1), 45–51.

44 P. G. Jones, *Acta Crystallogr., Sect. B*, 1980, **36**, 2775–2776.

45 J. C. Vickery, M. M. Olmstead, E. Y. Fung and A. L. Balch, *Angew. Chem., Int. Ed. Engl.*, 1997, **36**, 1179–1181.

46 B. Bovio, F. Bonati and G. Banditelli, *Inorg. Chim. Acta*, 1984, **87**, 25–33.

47 A. Hayashi, M. M. Olmstead, S. Attar and A. L. Balch, *J. Am. Chem. Soc.*, 2002, **124**, 5791–5795.

48 J. H. K. Yip and J. Prabhavathy, *Angew. Chem., Int. Ed.*, 2001, **40**, 2159–2162.

49 D. M. Stefanescu, H. F. Yuen, D. S. Glueck, J. A. Golen and A. L. Rheingold, *Angew. Chem., Int. Ed.*, 2003, **42**, 1046–1048.

50 G. Yang and R. G. Raptis, *Inorg. Chim. Acta*, 2003, **352**, 98–104.

51 S. D. Bunge, O. Just and W. S. Raees Jr., *Angew. Chem., Int. Ed.*, 2000, **39**, 3082–3084.

52 M. Nakamoto, A. Schier and H. Schmidbaur, *J. Chem. Soc., Dalton Trans.*, 1993, 1347–1348.

53 M. A. Bennett, L. L. Welling and A. C. Willis, *Inorg. Chem.*, 1997, **36**, 5670–5672.

54 M. Manassero, L. Naldini and M. Sansoni, *J. Chem. Soc., Chem. Commun.*, 1979, 385–386.

55 F. A. Vollenbroek, W. P. Bosman, J. J. Bour, J. H. Noordik and P. T. Beurskens, *J. Chem. Soc., Chem. Commun.*, 1979, 387–388.

56 J. W. A. van der Velden, J. J. Bour, F. A. Vollenbroek, P. T. Beurskens and J. M. M. Smits, *J. Chem. Soc., Chem. Commun.*, 1979, 1162–1163.

57 P. L. Bellon, F. Cariati, M. Manassero, L. Naldini and M. Sansoni, *Chem. Commun.*, 1971, 1423–1424.

58 J. W. A. van der Velden, J. J. Bour, W. P. Bosman and J. H. Noordik, *Inorg. Chem.*, 1983, **22**, 1913–1918.

59 V. W.-W. Yam, C.-L. Chan and K.-K. Cheung, *J. Chem. Soc., Dalton Trans.*, 1996, 4019–4022.

60 V. W.-W. Yam, E. C.-C. Cheng and Z.-Y. Zhou, *Angew. Chem., Int. Ed.*, 2000, **39**, 1683–1685.

61 T. K.-M. Lee, N. Zhu and V. W.-W. Yam, *J. Am. Chem. Soc.*, 2010, **132**, 17646–17648.

62 V. W.-W. Yam and E. C.-C. Cheng, *Top. Curr. Chem.*, 2007, **281**, 269–309.

63 SMART ver. 5.625 Software for the CCD Detector System, Bruker AXS Inc., Madison, WI, 2001.

64 SAINTPLUS ver. 6.22 Software for the CCD Detector System, Bruker AXS Inc., Madison, WI, 2001.

65 SADABS program for absorption correction using SMART CCD data based on the method of Blessing: R. H. Blessing, *Acta Crystallogr., Sect. A*, 1995, **51**, 33–38.

66 L. J. Farrugia, *J. Appl. Crystallogr.*, 1999, **32**, 837–838.

67 G. M. Sheldrick, *SHELXTL, ver. 6.10*, University of Göttingen, Germany, 1994.

68 A. L. Spek, *Acta Crystallogr., Sect. A*, 1990, **46**, C34.

69 G. Kresse and D. Joubert, *Phys. Rev. B*, 1996, **54**, 11169–11186.

70 J. P. Perdew, K. Burke and M. Ernzerhof, *Phys. Rev. Lett.*, 1996, **77**, 3865–3868.

71 G. Kresse and D. Joubert, *Phys. Rev. B*, 1999, **59**, 1758–1775.

72 R. Bader and P. MacDougall, *J. Am. Chem. Soc.*, 1984, **106**, 1594–1605.

73 G. Henkelman, A. Arnaldsson and H. Jónsson, *Comput. Mater. Sci.*, 2006, **36**, 254–360.

74 E. Sanville, S. D. Kenny, R. Smith and G. Henkelman, *J. Comput. Chem.*, 2007, **28**, 899–908.

75 W. Tang, E. Sanville and G. Henkelman, *J. Phys.: Condens. Matter*, 2009, **21**, 084204.

76 B. Chilukuri and T. R. Cundari, *J. Phys. Chem. C*, 2011, **115**, 5997–6003.